INORGANIC CHEMISTRY

FRONTIERS

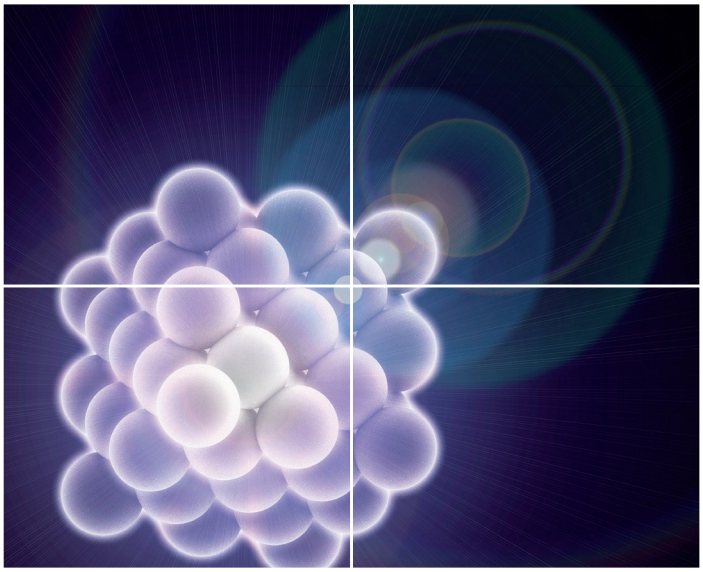

Accepted Manuscript

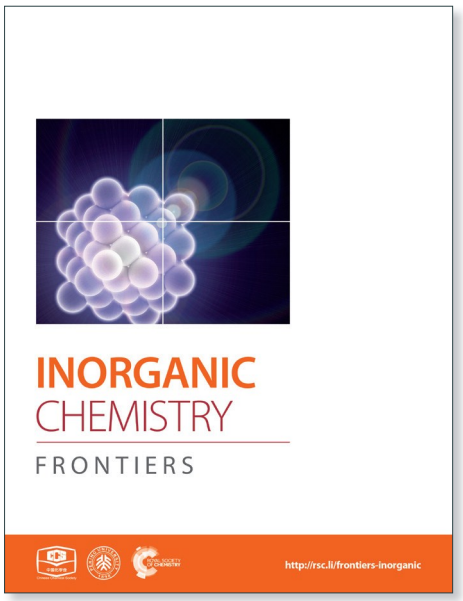

This is an *Accepted Manuscript*, which has been through the Royal Society of Chemistry peer review process and has been accepted for publication.

Accepted Manuscripts are published online shortly after acceptance, before technical editing, formatting and proof reading. Using this free service, authors can make their results available to the community, in citable form, before we publish the edited article. We will replace this *Accepted Manuscript* with the edited and formatted *Advance Article* as soon as it is available.

You can find more information about *Accepted Manuscripts* in the **Information for Authors**.

Please note that technical editing may introduce minor changes to the text and/or graphics, which may alter content. The journal's standard **Terms & Conditions** and the **Ethical guidelines** still apply. In no event shall the Royal Society of Chemistry be held responsible for any errors or omissions in this *Accepted Manuscript* or any consequences arising from the use of any information it contains.

Synthesis, crystal and electronic structure, and optical properties of two new chalcogenide-iodides: $Ba_3Q_4I_2$ (Q = S, Se)

Jian Wang, Kathleen Lee, Kirill Kovnir*

Department of Chemistry, University of California, Davis
One Shields Avenue, Davis, CA 95616, United States

Abstract

Two new ternary chalcogenide-iodides, $Ba_3S_4I_2$ and $Ba_3Se_4I_2$, were synthesized through high-temperature solid-state reactions, and their structures were determined via single-crystal X-ray diffraction. Both compounds are isostructural and crystallize in the monoclinic space group $C2/c$ (No. 15) with unit cell parameters of a = 14.507(4)/15.080(7) Å, b = 10.104(3)/10.400(5) Å, c = 8.206(2)/8.383(4) Å, β=101.847(4)/103.206(8)°, and Z = 4 for $Ba_3S_4I_2$/$Ba_3Se_4I_2$, respectively. The crystal structure of $Ba_3Q_4I_2$ (Q = S, Se) is constructed from Q_2^{2-} dumbbells and isolated I^{1-} anions, which are surrounded by Ba^{2+} cations. According to UV/Vis spectroscopy, $Ba_3S_4I_2$ is a semiconductor with a bandgap of 2.45(5) eV. Quantum-chemical calculations predict that $Ba_3S_4I_2$ and $Ba_3Se_4I_2$ are wide bandgap semiconductors with bandgaps of 2.50 and 2.06 eV, respectively. Electron localization function analysis of chemical bonding indicates covalent interactions in the Q_2^{2-} dumbbells.

Keywords: Crystal structure, chalcogenide; iodide, semiconductor, electronic structure, electron localization function.

Introduction

Metal chalcogenide-halides exhibit unique structural chemistry and properties, which are different from both metal chalcogenides and metal halides. The recent discovery of giant Rashba-type splitting in BiTeI,[1-2] spin density waves in La_2TeI_2,[3] high ionic conductivity and excellent thermoelectric properties in Ag-Te-*X* compounds (*X* = Cl, Br) are just few examples of the diversity in metal chalcogenide-halides.[4-8] In contrast to the ternary rare-earth- or transition metal-chalcogenide-halides, no ternary alkaline-earth-containing sulfide- or selenide-halides have been reported.[9-11] Only a few quaternary or higher order compounds have been reported in literature, such as $Ba_4Fe_2S_4I_5$,[12] $Ca_2LaGeS_4Cl_3$,[13] and $ABa_3Ga_5Se_{10}Cl_2$ (A = Cs, Rb, K).[14] Systematic investigations of the alkaline-earth metal–chalcogen–halogen systems may reveal new compounds and further rationalize the relationship between their structures and properties. In the current work, we report the first examples of two ternary compounds, $Ba_3S_4I_2$ and $Ba_3Se_4I_2$, which were synthesized through high-temperature reactions of elements. Detailed characterizations of the crystal structure, optical properties, and the electronic structure and bonding are reported.

Experimental

Synthesis. All preparation processes were handled in an argon-filled glovebox with the O_2 level <1 ppm. All starting materials were commercial grade and used as received: Ba (Sigma Aldrich, 99.9%), I_2 (Alfa Aesar, resublimed crystals, 99.9985%), S (Alfa Aesar, pieces, 99.999%), and Se (Alfa Aesar, powder 99.999%).

Polycrystalline $Ba_3Q_4I_2$ (*Q* = S, Se) samples were synthesized via two-step high-temperature reactions. In the first step, the reactants were loaded in stoichiometric ratios Ba:*Q*:I = 3:4:2 into carbonized silica ampoules, evacuated, and flame-sealed. The ampoules were placed in muffle

furnaces and heated from room temperature to 1073 K over a period of 20 hours, and then annealed at this temperature for 20 h, after which the furnace was turned off and the ampoules were cooled to room temperature. In the second step, the ampoules were opened in a glovebox, ground, resealed inside evacuated carbonized silica ampoules, and heated to 1073 K with the same heating rate, and annealed at 1073 K for an extended period of time, 144 h. The polycrystalline $Ba_3S_4I_2$ sample has a light yellow color, while $Ba_3Se_4I_2$ is dark-red. The $Ba_3S_4I_2$ sample was almost phase pure with tiny admixture of BaS according to powder X-ray diffraction (Figure S1), while the $Ba_3Se_4I_2$ samples always contained small admixtures of mainly BaSe and $BaSe_2$. All our attempts to synthesize single-phase samples of $Ba_3Se_4I_2$ by varying the temperature profile were unsuccessful. Both $Ba_3Se_4I_2$ and $Ba_3Se_4I_2$ are highly air and moisture sensitive, and will decompose in a few minutes under exposure to ambient atmosphere. Long time (2-3 months) storage of $Ba_3S_4I_2$ sample in the glovebox also resulted in partial sample decomposition.

X-ray powder diffraction. Powder X-ray diffraction (XRD) was carried out on a Rigaku Miniflex 600 diffractometer employing Cu-K_α radiation. Air-sensitive holders with Be or Kapton windows were used to prevent the decomposition of the samples during data collection.

Single crystal X-ray diffraction. Due to the air-sensitive nature of $Ba_3Q_4I_2$ (Q = S, Se), crystal selection and cutting were performed inside the glove box. Suitable crystals were quickly transferred to the dry nitrogen flow in the single crystal X-ray diffractometer. The datasets were collected at 90 K under a N_2 stream using a Bruker AXS SMART diffractometer with Mo-K_α radiation and an APEX-II CCD detector. The datasets were recorded as ω-scans with a 0.4° step width and integrated with the Bruker SAINT software package.[15] Multi-scan absorption corrections were applied.[15] The solutions and refinements of the crystal structures were carried

out using the SHELX suite of programs.[16] The final refinements were performed using anisotropic atomic displacement parameters for all atoms. A summary of pertinent information related to unit cell parameters, data collection, and refinements is provided in Table 1 and the atomic parameters and interatomic distances are provided in Tables 2 and 3. Further details of the crystal structure determination may be obtained from Fachinformations-zentrum Karlsruhe, D-76344 Eggenstein-Leopoldshafen, Germany, by quoting the depository numbers CSD-430355 ($Ba_3S_4I_2$) and CSD-430356 ($Ba_3Se_4I_2$).

Diffuse reflectance spectroscopy. UV-Vis diffuse reflectance spectra of $Ba_3S_4I_2$ were recorded using a Thermo Scientific Evolution 220 Spectrometer equipped with an integrating sphere. The reflectance data were converted to the Kubelka-Munk function, $f(R) = (1-R)^2(2R)^{-1}$. The sample was sealed inside a polypropylene bag under Ar atmosphere to prevent exposure to ambient conditions. An empty polypropylene bag was used for the baseline scan.

Quantum-chemical calculations. The electronic structure calculations and bonding analyses were carried out using the tight binding, linear muffin-tin orbital, atomic sphere approximation (TB–LMTO–ASA) program.[17] The Barth–Hedin exchange potential was employed for the LDA calculations. The radial scalar-relativistic Dirac equation was solved to obtain the partial waves. A basis set containing Ba(6*s*,5*d*,4*f*), I(5*p*), and S(3*s*,3*p*)/Se(4s,4p) orbitals with downfolded Ba(6*p*) and I(6*s*,5*d*) orbitals were used for $Ba_3S_4I_2$ and $Ba_3Se_4I_2$, respectively. The density of states (DOS), band structure, and electron localization function (ELF, η)[18-21] were calculated after converging the total energies on a *k*-mesh grid with 12×12×12 points with 476 irreducible *k*-points. The Paraview program was used to visualize the ELF isosurfaces.[22]

Results and Discussion

Structure Description

Both title compounds are isostructural and crystallize in the monoclinic space group *C*2/*c* (No. 15). For clarity only the crystal structure of $Ba_3S_4I_2$ is discussed (Figure 1).

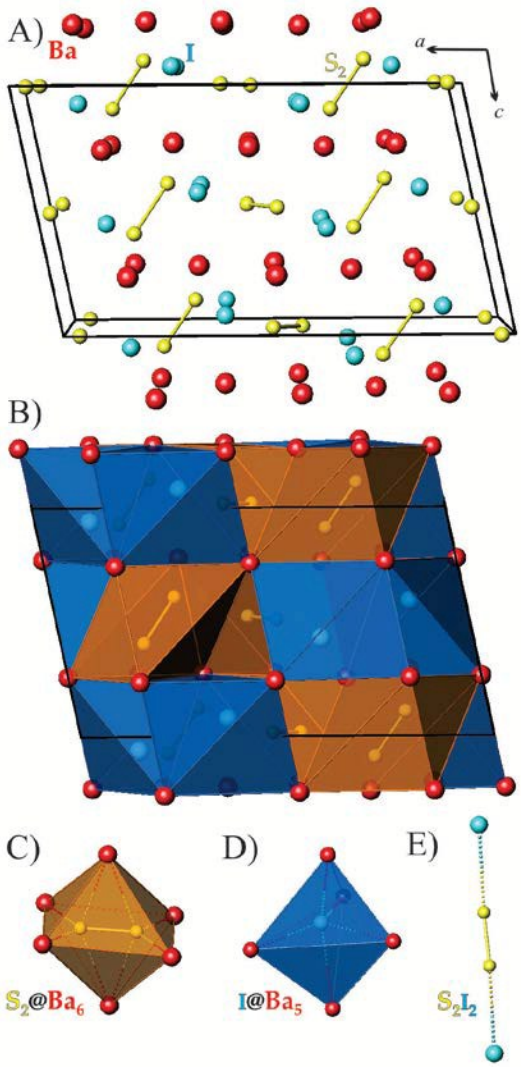

Figure 1. The crystal structure of $Ba_3S_4I_2$: A) general view of the unit cell; B) polyhedral representation of the unit cell; C) distorted Ba_6 octahedron around the S_2^{2-} dumbbell; D) distorted Ba_5 trigonal bipyramid around I^{1-}; E) a nearly linear S_2I_2 fragment. Ba: red; I: cyan; S: yellow. Unit cell is shown as black lines.

In the asymmetric unit of $Ba_3S_4I_2$ there are two Ba, one I, and two S sites that are crystallographically independent. All of the sulfur atoms are paired forming S_2^{2-} dumbbells (Figure 1). Each sulfur atom is additionally coordinated by four Ba atoms forming a distorted tetrahedron. Two such tetrahedra share a common edge in such a way that the S_2^{2-} dumbbells reside inside distorted Ba_6 octahedra (orange polyhedra in Figures 1B and 1C). Each iodine atom is surrounded by five Ba atoms forming a distorted trigonal bipyramid (blue polyhedra in Figures 1B and 1D). Both types of Ba atoms are surrounded by a distorted capped trigonal prisms composed of eight or nine atoms: Ba1 is surrounded by six sulfur atoms and three I atoms and Ba2 is coordinated to four sulfur atoms and four I atoms (Figure S2).

In $Ba_3S_4I_2$, the S–S distances are 2.107(2) and 2.121(2) Å, which are close to the sum of the corresponding Pauling radius of S (1.05 Å)[23] and comparable to S–S distances in barium polysulfides, such as BaS_2 (2.12 Å),[24] BaS_3 (2.08 Å),[25] $Ba_3Sb_2S_7$ (2.09 Å),[26] and $Sr_6Sb_6S_{17}$ (2.09 Å).[27] The Ba-S distances in $Ba_3S_4I_2$ (3.11-3.28 Å) are similar to the distances found in $Ba_3Sb_2S_7$ (3.14-3.35 Å),[26] $BaSb_2S_4$ (3.13-3.35 Å),[28] and $Ba_4Fe_2S_4I_5$ (3.20-3.30 Å).[12] The Ba-I distances (3.51-3.69 Å) are similar to the Ba-I distances in $Ba_4Fe_2S_4I_5$, which contains I atoms that are coordinated by four or five Ba atoms (3.51-3.73 Å).[12]

The bond distances in $Ba_3Se_4I_2$ exhibit similar trends as those in $Ba_3S_4I_2$ (Table 3). The Se-Se bonds in the Se_2^{2-} dimers, 2.384(3) and 2.394(3) Å, are much longer than the S-S bonds. These distances are close to the sum of the corresponding Pauling radius of Se (1.20 Å) [23] and comparable to Se-Se distances in elemental selenium and other reported compounds: 2.45 Å in Se_1,[29] 2.36 Å in Se_6,[30] 2.33-2.35 Å in Se_8,[31] 2.37 Å in $Ba_3Sb_2Se_7$,[26] and 2.37-2.42 Å in $Ba_4Sb_4Se_{11}$.[32] The Ba-Se distances in $Ba_3Se_4I_2$, 3.22-3.35 Å, are similar to the distances in various Ba selenides, such as 3.29 Å in BaSe,[33] 3.30-3.56 Å in $Ba_2Sb_2Se_5$,[34] 3.29-3.41 Å in

$Ba_4Sb_4Se_{11}$,[32] and 3.26-3.60 Å in $BaSb_2Se_4$.[35]. The Ba-I distances in $Ba_3Se_4I_2$, 3.51-3.77 Å, are longer than those in $Ba_3S_4I_2$, but are comparable to distances found in Ba_3SiI_2 (3.54-3.81 Å),[36] Ba_3GeI_2 (3.55-3.81 Å),[36] and $Ba_4Fe_2S_4I_5$ (3.51-3.73 Å).[12]

The shortest *Q*-I distances are nearly identical in both compounds with distances of 3.55 Å (*Q* = S) and 3.56 Å (*Q* = Se). Half of the Q_2^{2-} dumbbells are coordinated by iodine atoms forming almost linear Q_2I_2 fragments with angles of ∠I-*Q*-*Q* of 172.0° (*Q* = S) and 170.4° (*Q* = Se) (Figure 1E), while the remaining Q_2^{2-} dumbbells are coordinated by Ba atoms only.

$Ba_3Q_4I_2$ (*Q* = S, Se) are the first reported ternary mixed anions alkaline-earth sulfide- or selenide-halides. The isolated I^{1-} anions combined with Q_2^{2-} dumbbells, which have intrinsic covalent interactions, compensate the positive charge of the Ba^{2+} cations. $Ba_3Q_4I_2$ compounds exhibit two distict types of chemical bonding: covalent bonding in the Q_2^{2-} dumbbells and ionic bonding between cations and anions. Assuming +2 and –1 formal oxidation states for Ba and I, respectively, and a –1 oxidation state for all chalcogen atoms in the Q_2 dumbbells, total electroneutrality is achieved: $(Ba^{2+})_3(Q^{2-})_2(I^{1-})_2$. The ionic interactions among the Ba^{2+}, I^-, and S_2^{2-} ions result in a charge-balanced compound making $Ba_3S_4I_2$ a large band gap semiconductor, which was predicted from electronic structure calculations. Optical measurements and the translucent yellow color of $Ba_3S_4I_2$ further support such a description. Mercury-thallium chalcogenides with compositions similar to the title compounds, $Hg_3Q_4Tl_2$, also crystallize in *C*2/*c* space group. In these compounds, the chalcogen atoms are well separated from each other as Q^{2-} anions and instead of I^{1-} anions the Tl^{1+} cations are present, maintaining total electroneutrality as $(Hg^{2+})_3(Q^{2-})_4(Tl^{1+})_2$.[37]

UV −Vis Diffuse-Reflectance Spectroscopy

Solid-state UV-Visible Kubelka–Munk (KM) diffuse reflectance spectroscopy was employed to determine the bandgap of $Ba_3S_4I_2$. The UV−Vis spectrum exhibits apparent absorption edges around 490 nm (Figure 2). According to the Tauc plots, the indirect and direct band gaps of $Ba_3S_4I_2$ are 2.45(5) and 2.6(1) eV, respectively (Figure 2, bottom). The calculated value of the direct bandgap depends on the range selected for the linear fit, which resulted in high standard deviations. This result is in good agreement with the observed yellow-translucent color and calculated direct bandgap of 2.50 eV (*vide infra*). The combination of spectroscopic and computational approaches indicates that $Ba_3S_4I_2$ is a wide bandgap semiconductor.

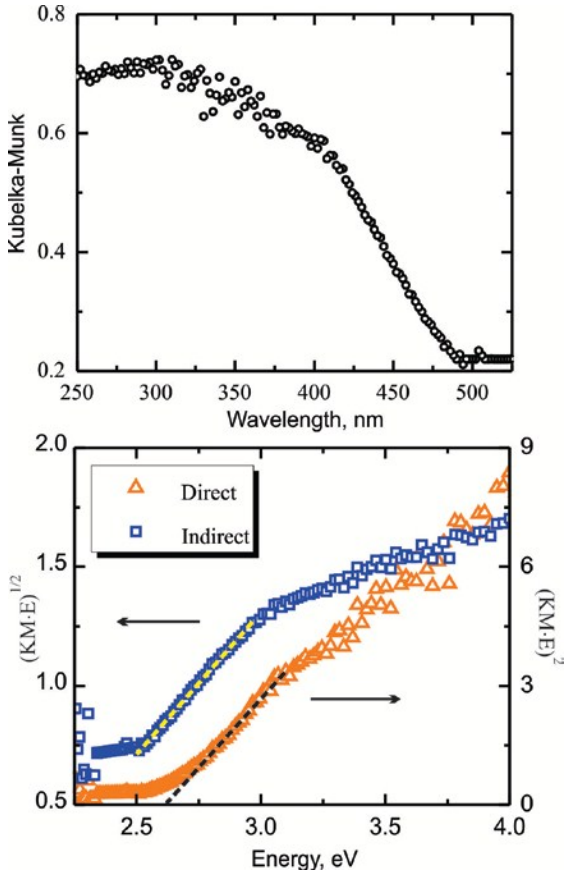

Figure 2. (Top) Solid-state UV-Visible Kubelka-Munk diffuse reflectance spectrum of $Ba_3S_4I_2$. (Bottom) Tauc plots for allowed direct (orange triangles) and indirect (blue squares) transitions.

Electronic Structure

Quantum chemical calculations show that both compounds are wide bandgap semiconductors with bandgaps of 2.50 and 2.06 eV for $Ba_3S_4I_2$ and $Ba_3Se_4I_2$, respectively (Figure 3, left). Calculations suggest that $Ba_3S_4I_2$ is a direct bandgap semiconductor, while $Ba_3Se_4I_2$ is an indirect bandgap semiconductor. $Ba_3S_4I_2$ has direct bandgaps of 2.50 eV at both the *L* and *Z* points of the Brillouin zone. Unlike $Ba_3S_4I_2$, $Ba_3Se_4I_2$ has an indirect bandgap of 2.06 eV with a direct bandgap of slightly higher energy (2.18 eV) at the *V* point. The direct transitions for $Ba_3Se_4I_2$ at the *L*, *Z*, and *Γ* points, 2.20, 2.27, and 2.26 eV, respectively, are very similar in energy to the energy difference at the *V* point.

Elemental projections of the density of states diagram (Figure 3, right) indicate that for both compounds, the states near the top of the valence band are composed from orbital contributions from all three elements, with dominating contributions from S (or Se) and I. Contributions from Ba orbitals dominate in the states at the conduction band at energies > +4 eV. The bottom of the conduction band is composed of two sharp peaks, which are essentially S (or Se) orbitals with minimal contributions from Ba and I.

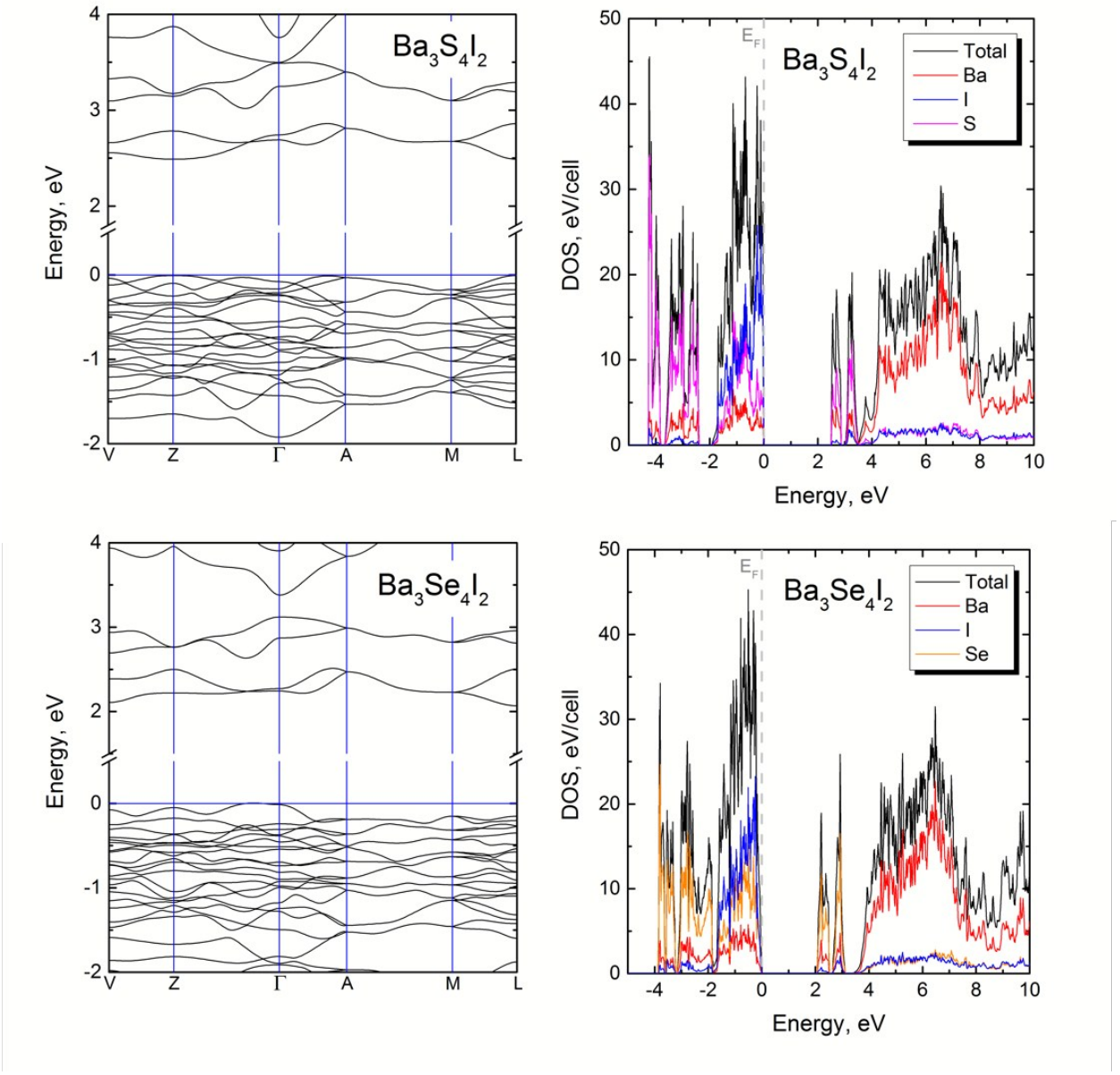

Figure 3. Band structures (left) and density of states (DOS) (right) for $Ba_3S_4I_2$ (top) and $Ba_3Se_4I_2$ (bottom).

Chemical bonding in $Ba_3Q_4I_2$ was analyzed with the help of electron localization function (ELF) analysis. The bonding analysis confirmed the expected covalent *Q*-*Q* bonding for the Q_2

dumbbells (attractor ①) with torus-like attractors on the terminal *Q* atoms (Figure 4). Similar torus-like distributions for ELF were found for the S_2^{2-} units in $Ba_3Sb_2S_7$.[26] According to Zintl or Lewis descriptions the Q^{1-} atoms in the isolated Q_2^{2-} dumbbells should have three electron lone pairs, and the spatial arrangements of those lone pairs should conform with $D_{\infty h}$ local symmetry. The observed torus-like arrangement is in accordance with those expectations. Similar ELF distributions were observed for the three lone-pairs located on O atoms in the OH^{1-} hydroxyl anions with $C_{\infty h}$ symmetry.[38] For the linear fragments with two terminal electron lone pairs, such as C_3^{4-}, a different, umbrella-like ELF distribution was reported. [39] In turn, for linear Sb_3^{7-} and isoelectronic ClF_2^{1-} where three electron lone pairs are expected on the central atoms, the ELF distribution is also torus-like.[20,40]

The ELF slices show deep minima surrounding the Ba and I atoms indicating no covalent bonds between the ions. However, significant structuring of both iodine and barium cores were observed, indicating the participation of 5th shell electrons of Ba and I in bonding interactions.

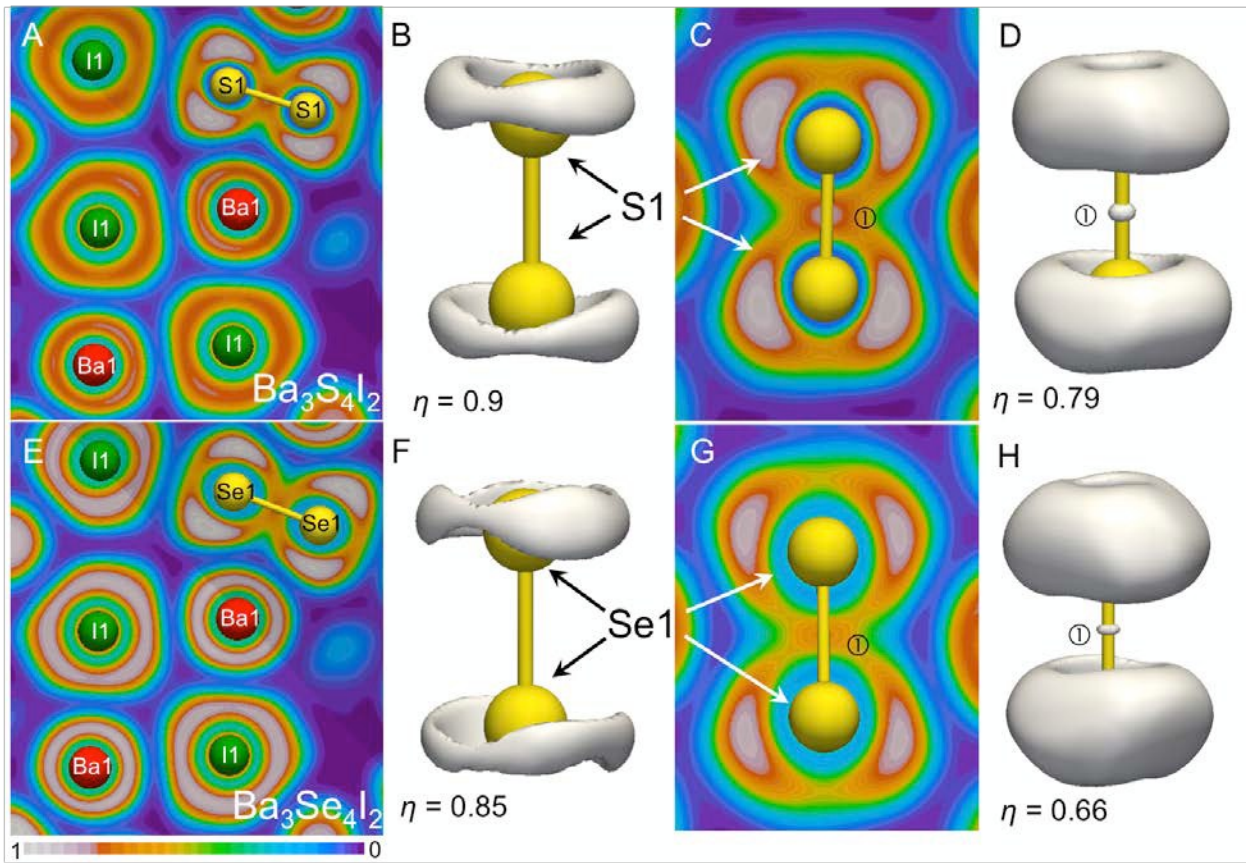

Figure 4. ELF slices and isosurfaces for $Ba_3S_4I_2$ (top) and $Ba_3Se_4I_2$ (bottom). (A and E) slices showing the ELF for Ba1, I, and the Q_2 dumbbells with the scale bar shown at the bottom left. (C and G) slices of the Q_2 dumbbells. (B, D, F, H) isosurfaces for the Q_2 dumbbell at different values of ELF, η, indicated in the figure.

Conclusions

Two new ternary chalcogenide iodides, $Ba_3S_4I_2$ and $Ba_3Se_4I_2$, have been synthesized and structurally characterized. Both compounds crystallize in the monoclinic space group *C*2/*c* (No. 15). The crystal structure of these compounds is comprised of Q_2^{2-} dumbbells and isolated I^{1-} anions surrounded by Ba^{2+} cations. $Ba_3S_4I_2$ is a wide bandgap semiconductor with an optical

bandgap of 2.45(5) eV, which is supported by electronic band structure calculations. ELF analyses indicate covalent bonding within the Q_2^{2-} dumbbells as well as polarization of the barium and iodine 5th electronic shells.

Acknowledgements

The authors would like to thank Prof. F. Osterloh for access to the UV-visible diffuse reflectance spectrometer. K.L. acknowledges the GAANN and ARCS fellowships. This research is supported by the U.S. Department of Energy, Office of Basic Energy Sciences, Division of Materials Sciences and Engineering under Award DE-SC0008931.

References

1 K. Ishizaka, M. S. Bahramy, H. Murakawa, M. Sakano, T. Shimojima, T. Sonobe,K. Koizumi, S. Shin, H. Miyahara,A. Kimura, K. Miyamoto, T. Okuda, H. Namatame, M. Taniguchi, R. Arita, N. Nagaosa, K. Kobayashi, Y. Murakami, R. Kumai, Y. Kaneko, Y. Onose, Y. Tokura, *Nat. Mater.*, 2011, **10**, 521-526.

2 J. S. Lee, G. A. H. Schober, M. S. Bahramy, H. Murakawa, Y. Onose, R. Arita, N. Nagaosa, Y. Tokura, *Phys. Rev. Lett.*,2011, **107**, 117401.

3 M. Ryazanov, A. Simon, H. Mattausch, *Inorg. Chem.*, 2006, **45**, 10728-10733.

4 T. Nilges, S. Nilsen, A. Pfitzner, T. Doert, P. Böettcher, *Chem. Mater.*, 2004, **16**, 806-812.

5 T. Nilges, C. Dreher, A. Hezinger, *Solid. State. Sci*., 2005, **7**, 79-88.

6 S. Lange, T. Nilges, *Chem. Mater.*, 2006, **18**, 2538-2544.

7 S. Lange, M. Bawohl, D. Wilmer, H. W. Meyer, H. D. Wiemhöefer, T. Nilges, *Chem. Mater.*, 2007, **19**, 1401-1410.

8 T. Nilges, O. Osters, M. Bawohl, J. L. Bobet, B. Chevalier, R. Decourt, R. Weihrich, *Chem. Mater.*, 2010, **22**, 2946-2954.

9 P. M. Carkner, H. M. Haendler, *J. Solid State Chem.*, 1976, **18**, 183-189.

10 C.M. Schurz, S. Frunder, T. Schleid, *Eur. J. Inorg. Chem.* 2013, 2923-2929.

11 M. Larres, I. Pantenburg, G. Meyer, *Z. Anorg. Allg. Chem.* 2013, **639**, 2744-2747.

12 D.L. Gray, G.-J. Long, F. Grandjean, R.P. Hermann, J.A. Ibers, *Inorg. Chem.*, 2008, **47**, 94-100.

13 R.L. Gitzendanner, F.J. DiSalvo, *Inorg. Chem.*, 1996, **35**, 2623-2626.

14 P. Yu, L. J. Zhou, L. Chen, *J. Amer. Chem. Soc.*, 2012, **134**, 2227-2235.

15 Bruker APEX2; Bruker AXS Inc.: Madison, WI, 2005.

16 G.M. Sheldrick, *Acta Crystallogr. A*, 2008, **A64**, 112-122.

17 O. Jepsen, A. Burkhardt, O. K. Andersen, The Program TB-LMTO-ASA , Version 4.7, Max-Planck-Institut für Festkörperforschung, Stuttgart, Germany, 1999.

18 A. D. Becke, K. E. Edgecombe, *J. Chem. Phys.*, 1990, **92** , 5397-5403.

19 A. Savin, O. Jepsen, J. Flad, O. K. Andersen, H. Preuss, H. G. Von Schnering, *Angew. Chem.*, 1992, **104**, 186 -188; *Angew. Chem. Int. Ed. Engl.*, 1992, **31**, 187-188.

20 A. Savin, R. Nesper, S. Wengert, T. F. Fässler, *Angew. Chem.*, 1997, **109**, 1892-1918; *Angew. Chem. Int. Ed. Engl.*, 1997, **36**, 1808-1832.

21Yu. Grin, A. Savin, B. Silvi, in: *The Chemical Bond : Fundamental Aspects of Chemical Bonding* (Eds.: G. Frenking, S. Shaik), Wiley-VCH, Weinheim, 2014, p. 345–382.

22 a) Paraview: Parallel visualization application, version 4.1.0 64 bit; Sandia National Labs, Kitware Inc, Los Alamos National Labs: USA; http://paraview.org; b) A. I. Baranov, Visualization plugin for ParaView, Version 4.1.0, 2014.

23 L. Pauling, The Nature of the Chemical Bond, 3rd ed., Cornell University Press, Ithaca, NY, 1960.

24 I. Kawada, K. Kato, S. Yamaoka, *Acta Crystallogr B*, 1975, **31**, 2905-2906.

25 S. Yamaoka, J. T. Lemley, J. M. Jenks, H. Steinfink, *Inor.Chem.*, 1975, **14**, 129-131.

26 J. Wang, K. Lee, K. Kovnir, *Z. Anorg. Allg. Chem.*, 2015, **641**, 1087-1092.

27 K.-S. Choi, M. G. Kanatzidis, *Inorg. Chem.*, 2000, **39**, 5655-5662.

28 G. Cordier, C. Schwidetzky, H. Schaefer, *J. Solid State Chem.*, 1984, **54**, 84-88.

29 Y. Akahama, M. Kobayashi, H. Kawamura, *Phys Rev B.*, 1993, **47**, 20-26.

30 Y. Miyamoto, *J. Appl. Phys.*, 1980, **19**, 1813-1819.

31 P. Cherin, P. Unger, *Acta Crystallogr. B*, 1972, B***28***, 313-317.

32 G. Cordier, R. Cook, H. Schäfer, *Angew. Chem.* 1980, **92**, 310. *Angew. Chem. Int. Ed. Engl.*, 1980, **19**, 324-325.

33 Y.B. Lyskova, A.V. Vakhobov, *Inorg. Mater*., 1975, **11**, 1784-1785.

34 J. Wang, K. Lee, K. Kovnir, *J. Mater. Chem. C*, 2015, **3,** 9811-9818.

35 G. Cordier, H. Schäfer, *Z. Naturforsch. B*., 1979, **34**, 1053-1056.

36 S. Wengert, R. Nesper , *J. Solid State Chem.*, 2000, **152**, 460-465.

37 S. Johnsen, S. C. Peter, S. L. Nguyen, J.-H. Song, H. Jin, A. J. Freeman, M. G. Kanatzidis, *Chem. Mater.*, 2011, **23**, 4375-4383.

38 M. E. Tuckerman, D. Marx, M. Parrinello, *Nature*, 2002, **417**, 925-929.

39 D. A. Lang, J. V. Zaikina, D. D. Lovingood, T. E. Gedris, S. E. Latturner, *J. Am. Chem. Soc.*, 2010, **132**, 17523–17530.

40 Y. Hu, J. Wang, A. Kawamura, K. Kovnir, S.M. Kauzlarich, *Chem. Mater.*, 2015, **27**, 343-351.

Table 1. Selected crystal data and structure refinement parameters for $Ba_3Q_4I_2$.

Empirical formula	$Ba_3S_4I_2$	$Ba_3Se_4I_2$
Formula weight	794.06 g/mol	947.00 g/mol
CSD number	430355	430356
Temperature	90(2) K	
Radiation, wavelength	Mo-K_α, 0.71073 Å	
Crystal system	monoclinic	
Space group	*C*2/*c* (No. 15)	
Unit cell dimensions	a = 14.507(4) Å	a =15.080(7) Å
	b = 10.104(3) Å	b =10.400(5) Å
	c = 8.206(2) Å	c =8.383(4) Å
	β =101.847(4)°	β = 103.206(8)°
Unit cell volume	1177.3(5) $Å^3$	1280.0(11) $Å^3$
Z	4	
Density (*calc.*)	4.48 g/cm^3	5.09 g/cm^3
Absorption coefficient	15.81 mm^{-1}	25.27 mm^{-1}
Goodness-of-fit	1.07	1.05
Final R indices[a]	R_1 = 0.029	R_1 = 0.040
[$I > 2\sigma(I)$]	wR_2 = 0.051	wR_2 = 0.075
Final R indices[a]	R_1 = 0.040	R_1 = 0.057
[all data]	wR_2 = 0.056	wR_2 = 0.083

[a] $R_1 = \sum||F_o| - |F_c||/\sum|F_o|$; $wR_2 = [\sum[w(F_o^2 - F_c^2)^2]/\sum[w(F_o^2)^2]]^{1/2}$, and $w = 1/[\sigma^2F_o^2 + (A\cdot P)^2 + B\cdot P]$, $P = (F_o^2 + 2F_c^2)/3$; A and B are weight coefficients.

Table 2. Refined atomic coordinates and isotropic displacement parameters for $Ba_3Q_4I_2$.

Atom	Wyckoff	*x/a*	*y/b*	*z/c*	*S.O.F.*	U_{eq} (Å^2) [a]
			$Ba_3S_4I_2$			
Ba1	8*f*	0.32778(2)	0.08927(3)	0.25914(3)	1	0.00547(7)
Ba2	4*e*	0	0.17704(4)	¼	1	0.00585(9)
I1	8*f*	0.36677(2)	0.40252(3)	0.07541(4)	1	0.00734(8)
S1	8*f*	0.20128(8)	0.29103(12)	0.3998(2)	1	0.0073(2)
S2	8*f*	0.46625(8)	0.0928(1)	0.0035(2)	1	0.0067(2)
			$Ba_3Se_4I_2$			
Ba1	8*f*	0.32777(5)	0.09615(7)	0.25626(9)	1	0.0114(2)
Ba2	4*e*	0	0.1639(1)	¼	1	0.0119(3)
I1	8*f*	0.36657(6)	0.40283(8)	0.0708(1)	1	0.0137(2)
Se1	8f	0.19701(8)	0.2952(1)	0.3862(2)	1	0.0115(3)
Se2	8*f*	0.46253(8)	0.1015(1)	–0.0002(2)	1	0.0113(3)

[a] U_{eq} is defined as one third of the trace of the orthogonalized U_{ij} tensor.

Table 3. Selected interatomic distances (Å) in $Ba_3Q_4I_2$.

Atom pair	Distance (Å)	Atom pair	Distance (Å)
		$Ba_3S_4I_2$	
Ba1– S1	3.119(1)	Ba2– S1×2	3.145(1)
S1	3.156(1)	S2 ×2	3.224(1)
S1	3.276(1)	I1 ×2	3.5136(8)
S2	3.128(1)	I1 ×2	3.6921(7)
S2	3.188(1)	S1– S1	2.107(2)
S2	3.215(1)	S2– S2	2.121(2)
I1	3.5111(8)		
I1	3.6003(8)		
		$Ba_3Se_4I_2$	
Ba1– Se1	3.216(2)	Ba2– Se1 ×2	3.232(2)
Se1	3.303(2)	Se2 ×2	3.347(2)
Se1	3.341(2)	I1 ×2	3.506(2)
Se2	3.260(2)	I1 ×2	3.773(2)
Se2	3.279(2)	Se1– Se1	2.384(3)
Se2	3.351(2)	Se2– Se2	2.394(3)
I1	3.526(2)		
I1	3.654(2)		

TOC Image

Two new ternary chalcogenide-iodides, $Ba_3S_4I_2$ and $Ba_3Se_4I_2$, exhibit both covalent and ionic chemical bonding.